

Spatiotemporal model of a key step in endocytosis: SNX9 recruitment via phosphoinositides

Johannes Schöneberg^{†1}, Alexander Ullrich^{†1}, York Posor[‡], Volker Haucke[‡], Frank Noe^{†*}

December 10, 2021

Abstract

Clathrin mediated endocytosis (CME) is an ubiquitous cellular pathway that regulates central aspects of cell physiology such as nutrient uptake, modulation of signal transduction, synaptic transmission and membrane turn-over. Endocytic vesicle formation depends on the timed production of specific phosphoinositides and their interactions with various endocytic proteins. Recently, it has been found that phosphatidylinositol-3,4-bisphosphate (PI(3,4)P₂) produced by the class II phosphatidylinositol 3-kinase C2α plays a key role in the recruitment of the PX-BAR domain protein SNX9, which is proposed to play a role in the constriction of the endocytic vesicle neck [1]. Interestingly, SNX9 and its close paralog SNX18 are not fully specific to PI(3,4)P₂ but can also bind other phospholipids, in particular to PI(4,5)P₂, an abundant plasma membrane lipid required for the recruitment of many endocytic proteins. In order to understand the dynamical interplay between phospholipids and endocytic proteins, we developed a computational model of the temporal changes in the population of the phosphoinositide-associated endocytic proteins and their spatial distribution at a clathrin-coated pit (CCP). The model resolves single molecules in time and space, and incorporates the complex interplay of proteins and lipids, as well as their movement within the CCP. We find that the comparably small differences in lipid binding affinities of endocytic proteins are amplified by competition among them, allowing for the selective enrichment of SNX9 at late stage CCPs as a result of timed PI(3,4)P₂ production.

[†]: FU Berlin, Department of Mathematics and Computer Science, Arnimallee 6, 14195 Berlin, Germany

[‡]: Leibniz Institut für Molekulare Pharmakologie, Robert-Roessle-Strasse 10, 13125 Berlin, Germany

1: equal contribution

*: correspondance to frank.noe@fu-berlin.de

Introduction

Clathrin mediated endocytosis (CME) is a key process by which cells internalize surface proteins including nutrient and signalling receptors, adhesion proteins, or ion channels. CME can be divided into four steps, CCP nucleation at the plasma membrane, CCP invagination, dynamin-mediated scission of late stage CCPs and clathrin uncoating of the free vesicle. While many key players and interactions of this endocytic pathway have been studied intensively, we are just starting to understand the spatiotemporal regulation of CME. An important factor in CME are phosphoinositides and their timed formation by specific kinases and phos-

phatases [2, 3, 4]. Phosphatidylinositol-4,5-bisphosphate [PI(4,5)P₂] is known to play an important role in CME by associating with CCP components such as adaptor protein AP-2 and membrane curvature inducing proteins including epsins [5, 6]. Less is known about phosphoinositides other than PI(4,5)P₂ and their potential roles in regulating CME. The recent identification of PI3K C2α and its lipid product phosphatidylinositol-3,4-bisphosphate (PI(3,4)P₂) as regulators of CME suggests an interplay of two distinct PI-bisphosphate species, PI(4,5)P₂ and PI(3,4)P₂, in driving CME [1]. Formation of PI(3,4)P₂ appears to be spatiotemporally coupled to PI(4,5)P₂-mediated CCP assembly as recruitment of PI3K C2α depends on clathrin, which via early acting adaptors FCHo, AP-2, or CALM selectively associates with PI(4,5)P₂-rich membrane sites. Elevated levels of PI(3,4)P₂ might then facilitate the enrichment of PI(3,4)P₂-binding effector proteins, most notably SNX9 prior to dynamin-mediated endocytic vesicle fission. A prediction from these findings is that SNX9 is recruited to CCPs subsequent to PI3K C2α but preceding the burst of dynamin 2 recruitment. TIRF microscopy analysis of the timing of endocytic protein recruitment indeed revealed that accumulation of mCherry-SNX9 was delayed by about 20 s with respect to eGFP-PI3K C2α but clearly preceded the arrival of the majority of dynamin 2 [1], consistent with a prominent role for PI(3,4)P₂ in stabilizing SNX9 at endocytic sites. This time course of SNX9 arrival at CCPs coincides with a critical phase of the endocytic process during which extensive membrane remodelling must occur as a narrow stalk is formed that becomes a substrate for membrane fission by dynamin (and possibly other proteins such as epsins[7]). SNX9, in spite of its apparent dependence on PI(3,4)P₂ production by PI3K C2α did not display a strong preference for PI(3,4)P₂ over PI(4,5)P₂ *in vitro*. Since different endocytic proteins may compete for the same population of PIs *in vivo*, the protein-lipid population dynamics may be complex and cannot be predicted easily based on single binding affinity values.

In this study, we designed a theoretical reaction-diffusion model with single-molecule resolution, in order to grasp this complex interplay of proteins and lipids. Computer simulations of this model can trace population changes and spatial distribution of PI-binding proteins at CCPs depending on PI concentration. The model is parametrized to have a steady state with absolute protein copy numbers determined from proteomic studies[8] and uses published lipid binding affinities of the major PI-binding endocytic proteins[5, 9, 10, 11] (see Methods and [1] for details).

Methods

Single-particle reaction diffusion simulation model

In order to model the distribution and diffusion of phospholipids and endocytic proteins underneath the clathrin coat, a single-particle reaction-diffusion model of a single CCP was developed. Computer simulations of this model can trace phospholipid-dependent population changes at CCPs depending on PI concentration. The model is parametrized to have a steady state with absolute protein copy numbers determined from proteomic studies and uses published lipid binding affinities of the major PI-binding endocytic proteins (see Table S1). This model represents space in a coarse-grained manner, such that it is not able to resolve fine details such as protein crowding as nonuniform protein distributions reliably, but is rather suited to efficiently calculate the time-dependent population changes of proteins at the CCP. The simulation space consists of a hexagonal grid of 217 discrete simulation cells, representing a membrane patch of about 200 nm diameter (see Fig. 1a). In order to model a prototypical clathrin cage, a fixed arrangement of 54 intertwined clathrin triskelia was mapped on the grid (Fig. 1a). Each clathrin triskelion exposes three binding sites to clathrin-binding endocytic proteins underneath (Fig. 1b). In the simulation, the clathrin coat has the sole purpose of defining the positions of these binding sites. At any time, each simulation cell maintains the following pieces of information:

- Copy number of PI(3,4)P₂ and PI(4,5)P₂ molecules
- Copy number of membrane-associated proteins for each of the following proteins: SNX9, AP-2, FCHo2, CALM, Epsin.
- Number of clathrin binding sites, and which proteins are bound there, if any. Each protein copy in the simulation maintains the following data:
- The number of PI(3,4)P₂ or PI(4,5)P₂ molecules bound.

The simulation proceeds in discrete time steps of 0.01 ms. In each time step, all lipid molecules and all membrane-associated protein molecules can diffuse laterally, and can undergo “reactions”, corresponding to binding or unbinding events.

Diffusion:

Both phosphoinositides and membrane-associated proteins can diffuse laterally. Since each single copy of phosphoinositide and protein is represented as an explicit object, diffusion corresponds to jump events of lipids or proteins between neighboring simulation cells. The probability with which a jump may be attempted within a simulation time step is calculated from the diffusion constant, the simulation cell surface area, and the time step duration. For lipids, all jump attempts are executed. For proteins, the success of a jump event depends on the size of the protein and the occupancy of the target simulation cell. In this way, crowding effects are included in the model - proteins can only diffuse to places where sufficient physical space is vacant. Proteins do not diffuse while they are bound to clathrin. Any lipids bound to a protein are also not considered for independent

diffusional jumps, but will always move together with the associated protein.

Reactions:

Within each simulation cell, several types of binding or unbinding reactions may occur between clathrin, the endocytic proteins and phosphoinositides contained in the cell (Fig. 1c-e). Since the simulation proceeds by discrete time steps, one reaction event of each type is considered per time step and is executed with the probability $p = 1 - \exp(-k \text{ dt})$, where k is the rate and dt is the time step duration.

- Protein association: Endocytic proteins are recruited to the membrane from a small section of the cytosol 20nm above the membrane with a rate constant $k_{on,membrane}$ (Table S1). The number of proteins available per simulation cell for such a recruitment attempt is fixed by the bulk concentration (Table S1). A recruitment event is only executed, if the protein size can still be accommodated on the target cell.
- Protein dissociation: Membrane-associated proteins that are bound to neither phosphoinositide nor clathrin are only associated with their intrinsic affinity. Such a protein may dissociate with a dissociation rate defined by the intrinsic microscopic binding affinity, $K_{a,mem}$, (Table S1) and the binding rate. Upon dissociation, it is then removed from the simulation cell. The cytosolic population remains constant throughout the simulation. Membrane-associated proteins that bind at least one phosphoinositide or are bound to a clathrin binding site are not considered for dissociation. Such proteins must first lose their phosphoinositide and/or dissociate from clathrin before being considered for dissociation.
- Lipid binding: Phosphoinositide binding sites of any membrane-associated protein can bind free phosphoinositides present in the same simulation cell with a rate $K_{on,lipid}$ (Table S1).
- Lipid unbinding: Each binding site associated with a phosphoinositide can unbind this lipid with dissociation rates based on the binding rates and the affinities $K_{a,lip45}$, $K_{a,lipweak45}$, $K_{a,lip34}$ and $K_{a,lipweak34}$ (Table S1).
- Clathrin-Protein association: Proteins can bind to free clathrin binding sites in the same simulation cell with a rate $K_{on,clathrin}$ (Table S1). Each clathrin binding site can only associate with one protein at a time. The protein remains in the same simulation cell but is removed from the freely diffusing pool.
- Clathrin-Protein dissociation: Proteins associated to clathrin binding sites can dissociate with a rate according to the binding rate and the affinity $K_{a,clathrin}$ (Table S1). The protein remains in the same simulation cell and is returned to the freely diffusing pool.
- Production of PI(3,4)P₂ by PI3K C2 α : PI(3,4)P₂ is produced by phosphorylation from the implicit pool of PI(4)P. Since PI3K C2 α is associated with clathrin terminal domains, the reaction is conducted at clathrin binding sites with a rate k_{kinase} (Table S1) whose value

depends on the simulation parameter set used. Every such reaction event increments the local PI(3,4)P₂ lipid count by one. The production of PI(3,4)P₂ is only started after a simulation time of 10 s.

- Depletion of PI(4,5)P₂ by phosphatases: In some simulation parameter settings, we are considering the action of phosphatases that deplete the PI(4,5)P₂ pool with a rate of $k_{phosphatase}$ (Table S1) at every clathrin binding site.

All reactions are described by a on- and an off-rate. Since no sufficient experimental data was available to define all these rates, we extracted the binding affinities (or dissociation constants) from experimental data, and then set the absolute value of k_{on} arbitrarily. The effect of this arbitrary choice is that the kinetics, i.e. the speed at which equilibria or steady states are reached in our simulation is not predictive - in reality the equilibrium protein population could be reached faster or slower than in our simulations after the change of the lipid concentration. However, the equilibrium state itself, i.e. the number of membrane-associated proteins of any type for each given lipid concentration is well-defined based on experimentally-determined parameters and may be used to draw conclusions.

Simulation setup and basic parameters

An overview of all parameters used in the reference parameter set can be found in Table S1. The set is based on the model of a CCP having a diameter of about 100-150 nm and projected on a two-dimensional plane. The CCP is simulated on a hexagonal simulation area of about 200 nm diameter, discretized into 217 hexagonal simulation cells (see Fig. 1a), each having a radius of about 9.25 nm and a surface area of 222.5 nm^2 , yielding a total surface area of $0.064 \text{ } \mu\text{m}^2$. The model includes a regular hexagonal coat of 54 clathrin molecules, giving rise to a lattice of 162 N-terminal binding domains. These terminal binding domains are associated with specific simulation cells - such that a given simulation cell may have none, one or two terminal domains. We simulate the dynamics for a total time of 20s, in discrete time steps of $10 \text{ } \mu\text{s}$ duration each. The simulation starts with a concentration of 15,000 PI(4,5)P₂ phospholipids per μm^2 , uniformly distributed over the simulation area, resulting in 3 lipid molecules per cell. In the reference parameter set, the PI(4,5)P₂ concentration remains constant over the simulation time. The scheme is different for PI(3,4)P₂: Here the simulation starts with zero lipids. After 10s PI(3,4)P₂ is produced with a rate that elevates the PI(3,4)P₂ concentration within 5 s to the same level as the PI(4,5)P₂ concentration, consistent with expected turnover numbers of PI3Ks[12] and the copy number[8] and lifetime [1] of PI3K C2 α at CCPs. PI(3,4)P₂ lipids are only produced at clathrin terminal domains, because PI3K C2 α binds clathrin at this site[13].

Diffusion is modelled as a jump process between the grid cells, depending on the molecule’s diffusion constant and the area of grid cells of 222.5 nm^2 . For phospholipid diffusion, the experimental value of $3 \text{ } \mu\text{m}^2 \text{ s}^{-1}$ [14] was employed for both PI(4,5)P₂ and PI(3,4)P₂, yielding a jump rate of 13482.1 s^{-1} . For proteins, it is considered that diffusion in the cytosol is much faster than lateral membrane diffusion. Thus, the lateral diffusion constant of membrane-associated

proteins is determined by the diffusion of the bound phosphoinositides, here taken to be the lipid diffusion constant, divided by the number of binding sites of the protein. This calculation assumes that the lipids are sufficiently uncoupled such that their Brownian motion can be assumed to be uncorrelated *a priori*, but are *a posteriori* coupled because the protein has to move as a single unit. Whenever it was attempted to move a protein into a target cell (either through diffusion, or through binding to the membrane from the cytosol—see below), availability of sufficient space was tested. The probability with which such a move would be accepted was set to account for the actual space left in that particular cell. For example, if a cell can take four globular proteins of a certain size, and three are already residing inside the cell, the probability to successfully place a fourth one is very low because it is unlikely that the space at the randomly chosen insertion point is completely free of other particles causing overlaps. We have thus computed placement probabilities for proteins of different sizes, depending on the space already allocated on the target cell, and fitted this placement probability with the sigmoidal function $(1 + \exp(ar + b))^{-1}$ with r being the fraction of the simulation cell area already occupied, and a and b being fitting parameters (AP-2: $a=18.8$, $b=-2.7$; SNX9 & FCHo2: $a=13$, $b=-2.8$; Calm & Epsin: $a=9.3$, $b=-3.1$). Protein-membrane association parameters were computed based on published liposome binding experiments. In these experiments, molecules in the solution bind to a membrane and eventually bind different kind of lipids. With the model we derived in the section “Parameterisation of the protein binding model” (see below), we could differentiate between the two different processes of membrane binding and lipid binding and could use them separately in our microscopic model.

For all proteins but CALM, we assumed the macroscopic KD of $7.6 \text{ } \mu\text{M}$ of AP-2 for binding to PI(4,5)P₂[11]. For CALM, we used $5.8 \text{ } \mu\text{M}$ [9]. In our binding model, we assumed CALM and epsin to have one binding site, FCHo2 and SNX9 to have two equal binding sites, and AP-2 to have two strong and two weak binding sites[11]. The on-rate of lipid binding was set to 10000 s^{-1} . The cytosolic protein concentrations were set such that the protein numbers found under the clathrin coat in the steady state before the PI(3,4)P₂ increase matched the copy number of proteins found in CCVs, as described in a recent quantitative proteomic study[8]. Several other parameters (e.g. absolute values of rates) are free parameters that do not affect the steady states, provided that the parameters above are chosen as described (table S1). In order to show that the results of the simulation are robust with respect to parameter changes, the values of important parameters were varied, yielding a total of 270 different parameter sets that were all tested as to whether they yielded the same qualitative results. The results of this parameter sampling are reported in table S2 and Figure 3.

Parametrization of the protein-lipid binding model

We describe how experimentally-measured lipid binding affinities of endocytic proteins are transformed into their respective microscopic simulation parameters. The membrane

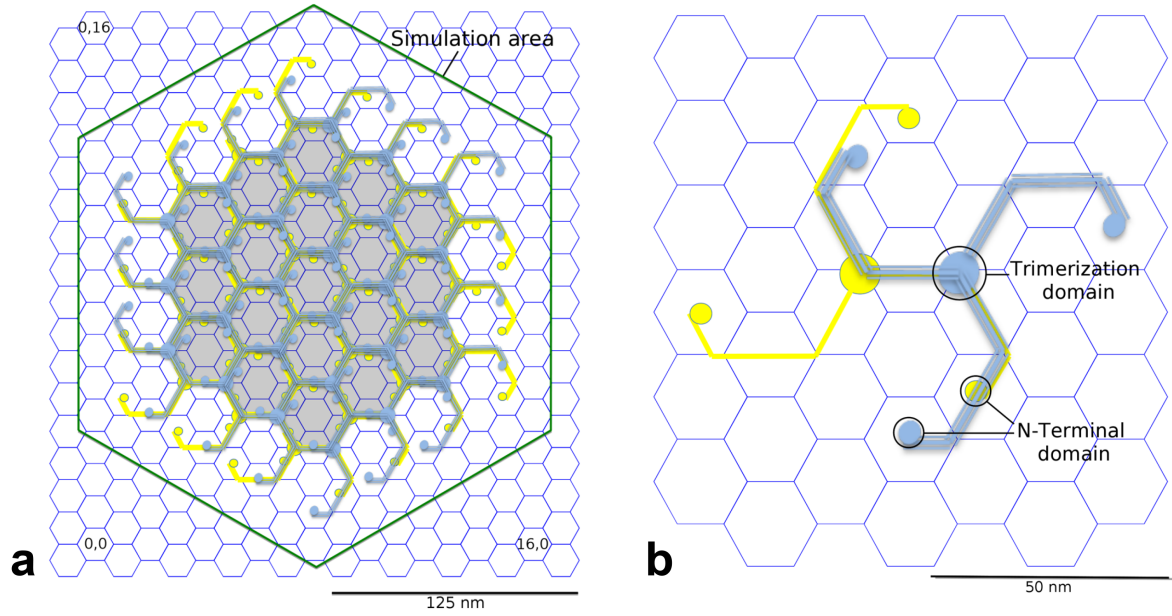


Figure 1: Illustration of the single-particle reaction-diffusion model of a CCP. a) Hexagonal simulation grid. The large green hexagon encribes the area simulated, consisting of 217 simulation cells (small blue hexagons). The yellow and blue structures represent 54 clathrin triskelia, with clathrin hubs shown as larger circles and binding sites shown as smaller circles. The shaded gray area is considered to be the area underneath the clathrin coat. b) Detailed view of two nearby clathrin triskelia (blue and yellow). The central sphere represents the hub of the clathrin triskelion, the terminal spheres represent the clathrin binding sites available to endocytic proteins in the same simulation cell. c) Summary of the reaction and binding processes occurring in simulation cells. d,e) Sketch of binding model for proteins with one/two phospholipid binding sites. Symbols: d: dissolved protein; O: membrane bound protein, no lipid bound; X: membrane bound protein, one lipid bound; XO: membrane bound protein, lipid in left one of two binding sites; OX: membrane bound protein, lipid in right one of two binding sites; XX: membrane bound protein, lipids in both of two binding sites; k_{mb} : protein-membrane binding rate; k_{ub} : protein-membrane unbinding rate; k_{lb} : protein-lipid binding rate; k_{lu} : protein-lipid unbinding rate. See Methods section and Table S1 for further details about the model and its parameterization.

dissociation constant of proteins is defined by:

$$K_D = \frac{[\text{Protein}][\text{Lipid}]}{[\text{Complex}]}$$

where $[\text{Protein}]$ is the volume concentration of the solvated protein (e.g. measured as mole per litre), $[\text{Complex}]$ is the surface concentration of all proteins that are associated to the membrane (either stably or transiently), and $[\text{Lipid}]$ is the surface concentration of lipids (e.g. measured in particles per nm^2). K_D is an experimentally-measurable dissociation

constant. When the lipid and complex concentrations are measured in the same unit, K_D will have the same unit as the protein concentration (e.g. mole per litre).

In order to convert the macroscopic entity K_D into microscopic simulation parameters, we must specify the dynamical model that the simulation uses to represent protein binding and dissociation events. Consider Fig. 1 c)-e) as an illustration of the binding dynamics. We consider a simulation cell which is a membrane patch with area A_{cell} . A hypothetical column of cytosol with height h is considered, yielding a

simulation cell volume V_{cell} (h and thus V_{cell} can be chosen arbitrarily - they are just needed as intermediate quantities for the calculation). The volume concentration of protein is thus given by:

$$[\text{Protein}] = \frac{n_d}{V_{cell}}$$

where n_d is the average copy number of solvated proteins considered in the simulation cell volume. We use the convention that all lipid and associated protein concentrations are measured in particle numbers per simulation cell area. Thus,

$$[\text{Lipid}] = n_{lipid}$$

is the number of lipids per surface area A_{cell} . As shown in Fig. 1 e), proteins can associate from the cytosol to state O, in which no phospholipid is bound, and can dissociate from state O to the cytosol. The fact that, depending on the settings of the rates k_{mb} and k_{mu} , proteins can be membrane-associated for some time even if no phospholipid is present represents the intrinsic membrane affinity of endocytic proteins. Usually, this intrinsic affinity is small and is controlled by the ratio k_{mb}/k_{mu} . From the associated state O, proteins may enter stably bound states (including at least one X), where the identifier X specifies which phospholipid binding sites are filled. We use the convention that a protein cannot dissociate from the membrane while at least one of the binding sites is filled with a phospholipid. This is based on the reasoning that pulling a phospholipid out of the membrane would be energetically extremely unfavorable. The mechanism of dissociation in our model is thus that phospholipids must first clear their binding sites, each with rate k_{lu} , before being able to dissociate with rate k_{mu} . The concentration of membrane-associated proteins is the total number of proteins in any lipid binding states on a surface A_{cell} . For proteins with a single binding site, this is:

$$[\text{Complex}] = n_O + n_X$$

where n_O counts membrane-associated proteins with empty binding sites and n_X counts membrane-associated proteins with filled binding sites. In proteins with two binding sites, we have the configurations:

$$\begin{aligned} [\text{Complex}] &= n_{OO} + n_{XO} + n_{OX} + n_{XX} \\ &= n_0 + 2n_1 + n_2 \end{aligned}$$

where n_k counts the number of membrane-associated proteins with k binding sites filled. Generally, when a protein has N binding sites, we have

$$[\text{Complex}] = \sum_{k=0}^N \binom{N}{k} n_k.$$

We write down the detailed balance equation for the protein association/dissociation reactions:

$$\begin{aligned} n_d k_{mb} &= n_0 k_{mu} \\ \frac{n_d}{n_0} &= \frac{k_{mu}}{k_{mb}} =: K_{d,mem} \end{aligned}$$

where we have defined the microscopic intrinsic membrane affinity $K_{d,mem}$. The detailed balance equation for the lipid binding/unbinding reactions are:

$$\begin{aligned} n_k n_{lipid} k_{lb} &= n_{k+1} k_{lu} \\ \frac{n_{lipid} n_k}{n_{k+1}} &= \frac{k_{lu}}{k_{lb}} =: K_{d,lip} \end{aligned}$$

for all $k = 0, \dots, N-1$, where we have defined the microscopic intrinsic lipid affinity $K_{d,lip}$. $K_{d,lip}$ varies depending on the protein and the type of lipid (PI(3,4)P₂ or PI(4,5)P₂). Combining all previous equations, we end up with the expression

$$\sum_{k=0}^N \binom{N}{k} \left(\frac{n_{lipid}}{K_{d,lip}} \right)^k = \frac{K_{d,mem} n_{lipid}}{K_D V_{cell}} \quad (1)$$

This permits the following approach to parametrize the binding model from experimental measurements of K_D :

1. Define a simulation cell height h to be used in the simulations, arriving at a cell volume V_{cell} .
2. Define a microscopic intrinsic protein-membrane affinity by setting $K_{d,mem}$.
3. Calculate $K_{d,lip}$ by solving Eq. (1) using the experimental concentration of n_{lipid} and the measured value of K_D .

For proteins with one binding site (CALM, Epsin), Eq. (1) has an explicit solution:

$$K_{d,lip}^{(1)} = \frac{n_{lipid}}{\frac{n_{lipid} K_{d,mem}}{K_{D,Calm} V_{cell}} - 1}.$$

For proteins with two equal binding sites (SNX9, FCHO₂), Eq. (1) has the following solution:

$$K_{d,lip}^{(2)} = \frac{n_{lipid}}{\sqrt{\frac{n_{lipid} K_{d,mem}}{K_D V_{cell}} - 1}}.$$

For AP-2, the situation is more complex. Experimentally, there is evidence that AP-2 has four binding sites. However, these are not equally strong but rather there are two conformations [11] associated with lipid binding affinities $K_{d,lip}^+$ and $K_{d,lip}^-$, respectively. Working out the lipid configuration for this case eventually yields the equation:

$$\begin{aligned} 1 + 2 \frac{n_{lipid}}{K_{d,lip}^+} + 2 \frac{n_{lipid}}{K_{d,lip}^-} + 2 \left(\frac{n_{lipid}}{K_{d,lip}^+} \right)^2 + 2 \left(\frac{n_{lipid}}{K_{d,lip}^-} \right)^2 \\ + 8 \frac{n_{lipid}^2}{K_{d,lip}^+ K_{d,lip}^-} + 10 \frac{n_{lipid}^3}{(K_{d,lip}^+)^2 K_{d,lip}^-} + 10 \frac{n_{lipid}^3}{K_{d,lip}^+ (K_{d,lip}^-)^2} \\ + 20 \frac{n_{lipid}^4}{(K_{d,lip}^+)^2 (K_{d,lip}^-)^2} = \frac{K_{d,mem} n_{lipid}}{K_D V_{cell}} \quad (2) \end{aligned}$$

To solve this formula for $K_{d,lip}^+$ and $K_{d,lip}^-$ we have to use additional information, compared to the equal binding site model in Equation 1, since we have now one additional unknown which renders our formula underdetermined without additional experimental input. Fortunately, in the case of AP-2, such additional input is available: The macroscopic dissociation constant K_D for AP-2 is known for the case where all four binding sites are operational [11]. We will refer here to that value by K_D^{++--} . Additionally the value $K_D^{+ + / /}$ is known, the dissociation constant for a mutant where the two weak binding sites have been mutationally inactivated [11]. Having these two constants, we now can firstly use $K_D^{+ + / /}$ in Equation 1 based on two binding sites,

which gives us a value for $K_{d,lip}^+$ and can then secondly use that value together with K_D^{++--} in Equation 2 to end up with a value for $K_{d,lip}^-$. The numerical values of the binding model parameters used are given in Table S1.

Results

A representative set of parameters for protein and lipid concentrations, binding affinities, rates and diffusion constants, was selected (Table S1) and the results are reported in Figure 2a. This data set uses an initially zero PI(3,4)P₂ concentration and a time-independent PI(4,5)P₂ concentration of approximately 15,000 lipids per μm^2 as PI 5-kinases are absent from assembled CCPs or coated vesicles[15]. The time-independent PI(4,5)P₂ concentration is a conservative assumption as several PI(4,5)P₂-specific phosphatases have been shown to be present in endocytic CCPs[16, 17], potentially resulting in progressive PI(4,5)P₂ hydrolysis.

With these lipid concentrations, the simulation reaches a steady state with a strong population of PI(4,5)P₂ binders such as AP-2, but only few SNX9 molecules associated with CCP membranes (Fig. 2a, top). Based on the experimentally-determined time course of PI3K C2 α recruitment to CCPs[1] we analysed the effects of increasing the PI(3,4)P₂ concentration in the simulation with respect to the concentration of the major endocytic PI binding proteins underneath the clathrin coat. Strikingly and consistently, SNX9 was the only endocytic protein which prominently enriched at CCPs concomitant with rising levels of PI(3,4)P₂, whereas other endocytic PI-binding proteins such as AP-2, FCHo, CALM, or epsin exhibited comparably minor changes during the simulated time course of 20 s (Fig. 2a).

Strong PI(3,4)P₂-dependent SNX9 recruitment occurs despite the conservative assumption that SNX9 binds to PI(3,4)P₂ and PI(4,5)P₂ equally well (Table 1b). This indicates that competition of different proteins for lipids plays an important role. Other proteins strongly favor PI(4,5)P₂ binding over PI(3,4)P₂ binding, especially AP-2 and Epsin. These proteins therefore win the competition for PI(4,5)P₂ lipids. This competition in turn acts as an amplification of the PI(3,4)P₂ signal for SNX9 recruitment, which is the only protein that can bind PI(3,4)P₂ sufficiently well to be sensitive to this signal. This is indeed confirmed by control simulations in the absence of competing endocytic proteins resulting in a much weaker response of the SNX9 population to increased PI(3,4)P₂ levels (see Fig. 3 bottom).

But why does SNX9 bind both PI(3,4)P₂ and PI(4,5)P₂ rather than being specific to PI(3,4)P₂ only? To explore this we ran a control simulation in which SNX9 is assumed to be PI(3,4)P₂-specific with no more than basal affinity for PI(4,5)P₂. Fig. 2b shows that in this case, PI(3,4)P₂ remains to serve as a strong signal for SNX9 recruitment, providing a large relative increase of the SNX9 population at the CCP. However, the absolute copy number of SNX9 molecules at the CCP are comparably low and remain insufficient for assembly of a closed PX-BAR domain ring around the neck of nascent late stage CCP. This observation provides a rational basis for its biochemical behaviour in lipid binding assays [1]. Thus, it appears that PI(4,5)P₂ is important for ensuring a basal concentration of SNX9 proteins. The production of PI(3,4)P₂ in this scenario “tips the scale” towards a selective amplification of SNX9 enrichment to reach a number sufficient to drive the endocytic reaction forward.

To test the robustness of our results, we performed simulations on varying PI concentrations and binding affinities, yielding a total of 270 different parameter combinations. In all combinations, increased PI(3,4)P₂ synthesis induced a robust increase in the levels of SNX9 (Fig. 3, Table S2).

Discussion

The present results suggest a mechanistic interpretation of the experimental results of Ref. [1] that is not apparent from the biochemical data alone. Limited numbers of phospholipids and lipid-binding proteins interact in a confined space, giving rise to a dynamic and competitive system with two surprising properties: (1) The activity of PI(3,4)P₂ is amplified as a result of competition of proteins for different types of lipids. (2) The limited specificity of SNX9, i.e. its ability to bind to both PI(3,4)P₂ and PI(4,5)P₂ is important for ensuring a sufficient total copy number of SNX9 molecules at a maturing CCP. The production of PI(3,4)P₂ can therefore be understood as a signal that tips the scales of a system that is already poised for progression.

Important open questions remain. In particular it is unclear how SNX9 recruitment is controlled not only in time but also in space and whether its enrichment at the CCP neck is compatible with the presumed localization of PI3k C2 α and its lipid product PI(3,4)P₂. A SNX9-coated neck may act as a molecule sling facilitating the constriction of the vesicle neck [18, 19, 20, 21].

References

- [1] Posor, Y. *et al.* Spatiotemporal Control of Endocytosis by Phosphatidylinositol 3,4-Bisphosphate. *Nature* **499**, 233–237 (2013).
- [2] Zoncu, R. *et al.* Loss of endocytic clathrin-coated pits upon acute depletion of phosphatidylinositol 4,5-bisphosphate. *Proceedings of the National Academy of Sciences of the United States of America* **104**, 3793–8 (2007).
- [3] Loerke, D. *et al.* Cargo and dynamin regulate clathrin-coated pit maturation. *PLoS biology* **7**, e57 (2009).
- [4] Krauss, M., Kukhtina, V., Pechstein, A. & Haucke, V. Stimulation of phosphatidylinositol kinase type I-mediated phosphatidylinositol (4,5)-bisphosphate synthesis by AP-2 μ -cargo complexes. *Proceedings of the National Academy of Sciences of the United States of America* **103**, 11934–11939 (2006).
- [5] Henne, W. M. *et al.* FCHo proteins are nucleators of clathrin-mediated endocytosis. *Science (New York, N. Y.)* **328**, 1281–4 (2010).
- [6] Cocucci, E., Aguet, F., Boulant, S. & Kirchhausen, T. The First Five Seconds in the Life of a Clathrin-Coated Pit. *Cell* **150**, 495–507 (2012).
- [7] Boucrot, E. *et al.* Membrane Fission Is Promoted by Insertion of Amphipathic Helices and Is Restricted by Crescent BAR Domains. *Cell* **149**, 124–136 (2012).

- [8] Borner, G. H. H. *et al.* Multivariate proteomic profiling identifies novel accessory proteins of coated vesicles. *The Journal of Cell Biology* **197**, 141–160 (2012).
- [9] Ford, M. G. *et al.* Simultaneous binding of PtdIns(4,5)P₂ and clathrin by AP180 in the nucleation of clathrin lattices on membranes. *Science (New York, N.Y.)* **291**, 1051–5 (2001).
- [10] Ford, M. G. J. *et al.* Curvature of clathrin-coated pits driven by epsin. *Nature* **419**, 361–6 (2002).
- [11] Jackson, L. P. *et al.* A large-scale conformational change couples membrane recruitment to cargo binding in the AP2 clathrin adaptor complex. *Cell* **141**, 1220–9 (2010).
- [12] Carpenter, C. L. *et al.* Purification and characterization of phosphoinositide 3-kinase from rat liver. *Journal of Biological ...* **26**, 19704–19711 (1990).
- [13] Gaidarov, I., Krupnick, J. G., Falck, J. R., Benovic, J. L. & Keen, J. H. Arrestin function in G protein-coupled receptor endocytosis requires phosphoinositide binding. *The EMBO journal* **18**, 871–81 (1999).
- [14] Almeida, P. F. F., Vaz, W. L. C. & Thompson, T. E. Lipid diffusion, free area, and molecular dynamics simulations. *Biophysical journal* **88**, 4434–8 (2005).
- [15] Antonescu, C. N., Aguet, F., Danuser, G. & Schmid, S. L. Phosphatidylinositol-(4,5)-bisphosphate regulates clathrin-coated pit initiation, stabilization, and size. *Molecular biology of the cell* **22**, 2588–600 (2011).
- [16] Perera, R. M., Zoncu, R., Lucast, L., De Camilli, P. & Toomre, D. Two synaptojanin 1 isoforms are recruited to clathrin-coated pits at different stages. *Proceedings of the National Academy of Sciences of the United States of America* **103**, 19332–7 (2006).
- [17] Nakatsu, F. *et al.* The inositol 5-phosphatase SHIP2 regulates endocytic clathrin-coated pit dynamics. *The Journal of cell biology* **190**, 307–15 (2010).
- [18] Shin, N. *et al.* SNX9 regulates tubular invagination of the plasma membrane through interaction with actin cytoskeleton and dynamin 2. *Journal of cell science* **121**, 1252–63 (2008).
- [19] Yarar, D., Waterman-Storer, C. M. & Schmid, S. L. SNX9 couples actin assembly to phosphoinositide signals and is required for membrane remodeling during endocytosis. *Developmental cell* **13**, 43–56 (2007).
- [20] Lundmark, R. & Carlsson, S. R. SNX9 - a prelude to vesicle release. *Journal of cell science* **122**, 5–11 (2009).
- [21] Ferguson, S. *et al.* Coordinated actions of actin and BAR proteins upstream of dynamin at endocytic clathrin-coated pits. *Developmental cell* **17**, 811–22 (2009).
- [22] Höning, S. *et al.* Phosphatidylinositol-(4,5)-bisphosphate regulates sorting signal recognition by the clathrin-associated adaptor complex AP2. *Molecular cell* **18**, 519–31 (2005).
- [23] Itoh, T. *et al.* Role of the ENTH domain in phosphatidylinositol-4,5-bisphosphate binding and endocytosis. *Science (New York, N.Y.)* **291**, 1047–51 (2001).

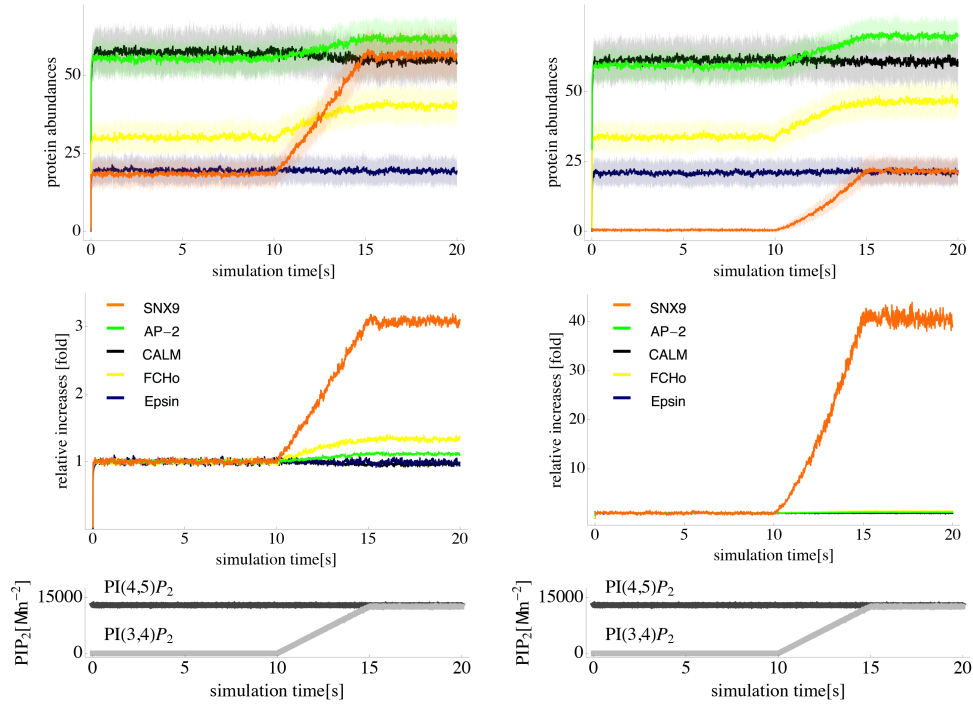


Figure 2: Spatiotemporal regulation of CME by PI3K C2 α -mediated PI(3,4)P₂ synthesis to recruit SNX9. a) Simulated endocytic protein abundances underneath the clathrin coat of a 2D-projected CCP over time. Averaged protein copy numbers (solid lines) \pm SD (shaded vertical bars; $n = 64$ simulation runs) are shown (top). Ratio of protein copy numbers normalized to those at time $t = 10$ s (middle). Concentration profile of PI(3,4)P₂ and PI(4,5)P₂ (bottom). Simulation is divided in 3 phases: equilibration phase (0 s - 10 s): constant PI(4,5)P₂ (middle). Concentration profile of PI(3,4)P₂ and PI(4,5)P₂ (bottom). Simulation is divided in 3 phases: equilibration phase (0 s and zero PI(3,4)P₂ level; rising phase (10 s-15 s): PI(3,4)P₂ is elevated to the level of PIP(4,5)P₂; equilibration phase (15 s-20 s). SNX9 copy numbers are selectively increased in response to PI(3,4)P₂ production to a value sufficient for formation of a ring around the CCP. Relevance of PI(4,5)P₂ affinity for the recruitment of SNX9 is tested by a control simulation where SNX9 binds exclusively PI(3,4)P₂ b). While SNX9 is strongly recruited to the membrane in both cases (a+b), the scenario in which SNX9 has no PI(4,5)P₂ affinity (b), does not reach a sufficient SNX9 level to form a ring around the CCP. This can be explained by the fact that PI(3,4)P₂ acts as an amplifier that multiplies the available SNX9 concentration with a certain factor, and thus needs to start from a base level significantly above zero to reach a substantial target value. Thus, SNX9's affinity to PI(4,5)P₂ is essential.

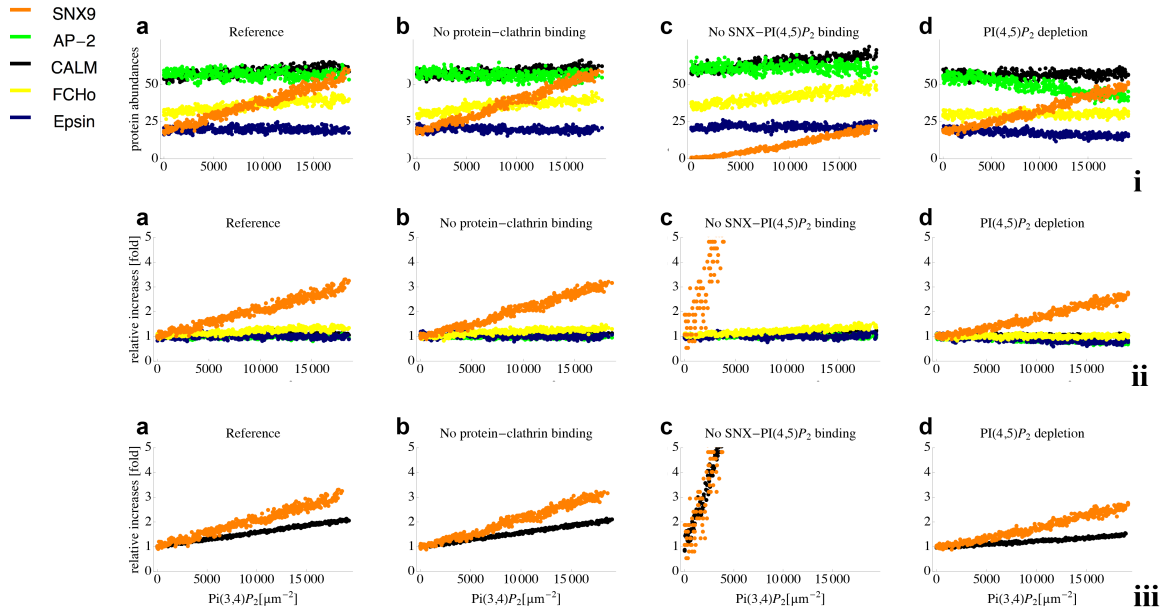


Figure 3: Sensitivity of CCP protein concentrations on the $\text{PI}(3,4)\text{P}_2$ lipids concentration. $\text{PI}(3,4)\text{P}_2$ is the main parameter for controlling the SNX9 concentration at the CCP, while other proteins exhibit little sensitivity on the $\text{PI}(3,4)\text{P}_2$ concentration. This can already be anticipated from Fig 2a, where it is seen that the SNX9 population essentially follows the $\text{PI}(3,4)\text{P}_2$ increase, while the other proteins remain mostly at the same population. To demonstrate this dependency more clearly, we have taken the simulated time traces of CCP protein numbers (e.g. Fig 2a), and, irrespective of the actual time, plotted each point of the time trace in a coordinate system showing the $\text{PI}(3,4)\text{P}_2$ concentration on the x-axis and the protein population on the y-axis. For visual clarity only data points from simulation times from $t=10\text{s}$ to $t=15\text{s}$ were used as the $\text{PI}(3,4)\text{P}_2$ concentration was constant during other times. Row i shows absolute protein numbers, Rows ii and iii show the relative increase of the protein number by dividing the absolute number by its value at $[\text{PI}(3,4)\text{P}_2]=0$. The columns a,b,c,d correspond to different choices of simulation parameters, thereby summarizing the results of 270 simulation settings with different parameter combinations in a simple way. Four cases are distinguished here. Compared to the reference parameter set (a), the other panels have parameter sets that are different from the reference set by one setting. b) Protein-Clathrin affinity was set to zero. c) $\text{PI}(4,5)\text{P}_2$ affinity to SNX9 was set to zero; d) The $\text{PI}(4,5)\text{P}_2$ concentration is reduced to half its initial value rather than remaining constant; In all scenarios, a clear sensitivity of SNX9 to the $\text{PI}(3,4)\text{P}_2$ concentration is seen, and the sensitivity of SNX9 population upon changes in $\text{PI}(3,4)\text{P}_2$ is always stronger than the sensitivity of other proteins to $\text{PI}(3,4)\text{P}_2$. Other proteins show very little sensitive to $\text{PI}(3,4)\text{P}_2$. In row iii, the relative change of SNX9 in the same conditions as in row ii (orange) is compared to a control simulation (black), where only SNX9 and no other phospholipid-binding protein was in the system. It is seen that in cases a, b, and c, SNX9 shows a much stronger response to changes in $\text{PI}(3,4)\text{P}_2$ concentrations when other proteins are present than when they are not present - the SNX9 number is approximately tripled rather than doubled. This indicates that $\text{PI}(3,4)\text{P}_2$ is not an independent regulator of endocytosis, but that the regulation depends on the competing interactions of proteins with the shared lipid pool.

a)	SNX9	AP-2	CALM	FCho2	Epsin
copy number ¹	7	54	54	33	21
footprint [nm ²] ²	34.25	84.5	8.46	83.6	9.8
# lipid bind. sites	2	4 (2s, 2w) ³	1	2	1
$K_{D,45}$ [μMol]		7.6 (30.0) ^{3,4}	5.8 ⁵		
$K_{D,34}/K_{D,45}$	1.0 ⁶	0.13 ⁴	0.22 ⁷	0.2 ⁸	0.33 ⁷
b)	SNX9	AP-2	CALM	FCho2	Epsin
k_{diff} [s ⁻¹]	6741.57	3370.79	13483.1	6741.57	13483.1
$conc_{cytosol}$ [1/ A_{sim}]	14.2	15.6	0.33	29.5	0.09
$K_{a,mem}$	0.11	5.19	5.2	0.11	4.03
$K_{a,lip45}$	3.32	0.21	9.98	3.32	9.98
$K_{a,lipweak45}$		0.0055			
$K_{a,lip34}$	3.32	0.06	2.17	1.64	2.47
$K_{a,lipweak34}$		0.0574			
$K_{a,clathrin}$	1.0	1.0	1.0	1.0	1.0
c)	D [μm ² /s] (experiment)		k_{diff} [s ⁻¹] (model)		
Phospholipids	3 ⁹		13483.1		
d)	time [s]	dt [μs]	cellsize [nm ²]	cellradius [nm]	
Global	20	10	222.3	9.25	
	$k_{on,membrane}$ [s ⁻¹]	$k_{on,lipid}$ [s ⁻¹]	$k_{on,clathrin}$ [s ⁻¹]		
Global	100000	10000	10		
e)	k_{kinase} [s ⁻¹]		$k_{phosphatase}$ [s ⁻¹]		
Clathrin N-terminal domain	0.8		(0.63)		

Table 1: Reference parameter set for the reaction-diffusion simulation. a) Experimentally-determined parameters used for the proteins simulated in the reaction-diffusion model, references are marked by superscripts and enlisted below. b) Protein-specific parameters used in the reaction-diffusion simulation that were either derived from (a), or computed as described in SI methods. c) Experimental and model parameters for the two phospholipids. d) Global simulation parameters. e) Kinase and phosphatase turnover rates. The phosphatase was not active in the reference parameter set, but only in some alternative parameter set considered in the parameter sampling (see Table S2). References: 1)[8], 2) PDB 2RAI, PDB 2xa7, PDB 1HFA, PDB 2V0o, PDB 1edu , 3) [11], 4) [22] , 5) [9], 6) [1], 7) [23], 8) [5], 9) [14]

Parameter	[SNX9] at t=10s	[SNX9] at t=20s	Δ SNX9	Δ others
CA = 0	18.7 \pm 14.2	82.4 \pm 46.4	4.4	1.02 \pm 0.14
CA = 1	19.4 \pm 13.6	82.2 \pm 45.0	4.2	1.04 \pm 0.14
CA = 100	19.0 \pm 13.1	81.9 \pm 43.9	4.3	1.03 \pm 0.14
PI(4,5)P ₂ Affinity = 0	2.6 \pm 2.9	57.2 \pm 37.0	22.0	1.04 \pm 0.15
PI(4,5)P ₂ Affinity = $\frac{1}{2}$	21.0 \pm 3.3	87.9 \pm 42.2	4.2	1.02 \pm 0.14
PI(4,5)P ₂ Affinity = 1	33.9 \pm 2.3	102.3 \pm 42.7	3.0	1.03 \pm 0.13
no PI(4,5)P ₂ depletion	19.2 \pm 13.6	83.0 \pm 45.1	4.3	1.15 \pm 0.06
PI(4,5)P ₂ depletion	19.0 \pm 13.5	81.3 \pm 44.7	4.3	0.92 \pm 0.09
[PI(4,5)P ₂] = 6.500/ μm^2	21.8 \pm 12.0	88.9 \pm 45.6	4.1	1.03 \pm 0.11
[PI(4,5)P ₂] = 13.000/ μm^2	17.2 \pm 13.5	81.8 \pm 47.1	4.8	1.02 \pm 0.15
[PI(4,5)P ₂] = 26.000/ μm^2	18.1 \pm 14.8	75.6 \pm 41.3	4.2	1.06 \pm 0.15
[PI(3,4)P ₂] = $\frac{1}{2}$ [PI(4,5)P ₂]	19.0 \pm 13.6	40.5 \pm 20.7	2.1	0.95 \pm 0.13
[PI(3,4)P ₂] = [PI(4,5)P ₂]	19.1 \pm 13.9	71.5 \pm 20.8	3.7	1.03 \pm 0.12
[PI(3,4)P ₂] = 2 [PI(4,5)P ₂]	19.0 \pm 13.4	134.4 \pm 26.1	7.1	1.11 \pm 0.11

Table 2: Overview of the parameter sampling results. Several uncertain simulation parameters were sampled in order to test whether our conclusions were robust with respect to parameter changes. For visual clarity, the 270 results are grouped according to equal values in individual parameters, each such group is associated with a row in the table. To ensure sufficient statistics, all 270 possible combinations of parameter values were simulated for 8 runs. The variation of the other parameters is described in terms of the standard deviation over all samples reported as a second number in table entries of columns 2,3, and 5. In the first column all sampled parameter values are shown. CA - The affinity of all proteins to bind the N-terminal domain of clathrin. PI(4,5)P₂ Affinity - The affinity of SNX9 to PI(4,5)P₂ in relation to PI(3,4)P₂. PI(4,5)P₂ depletion - the concentration of the lipid is decreased to half its starting value between t=10s and t=15s (or not). [PI(4,5)P₂] - concentration of the lipid in the simulation. [PI(3,4)P₂] = x[PI(4,5)P₂] - the target concentration of the lipid PI(3,4)P₂ in relation to the initial concentration of PI(4,5)P₂. The parameter values of the reference parameter set are highlighted in green. The parameters were assessed based on the properties listed in the first row, columns 2-5. In all scenarios, the concentration of SNX9 at t=10s (before addition of PI(3,4)P₂) was below the putative threshold of 40 to 50 copies required for ring formation (column 2). The only parameter with a significant influence on this quantity is the PI(4,5)P₂ affinity of SNX9. On the other hand (column 3) the concentration of SNX9 at t=20s increases substantially in all cases, and is usually well above 50. Higher PI(4,5)P₂ affinities and higher PI(3,4)P₂ concentrations have the most prominent effect on the final SNX9 concentration. While a certain SNX9 affinity to PI(4,5)P₂ is needed to ensure a baseline concentration of SNX9, the number of recruited SNX9 copies mainly depends on the amount of PI(3,4)P₂ produced (see also Fig 3). Column 4 reports the relative increase of SNX9 when dividing the SNX9 copy number after PI(3,4)P₂ production by the SNX9 copy number before the increase of PI(3,4)P₂. Low PI(4,5)P₂ concentrations also results in a high relative increase of SNX9, but are however starting from low initial SNX9 copy numbers and mostly do not reach sufficient total SNX9 copy numbers. Consequently, both the ability to bind to PI(4,5)P₂ and sufficient PI(3,4)P₂ levels are necessary to accumulate sufficient SNX9. Column 5 shows the relative change in copy numbers of the other proteins between t=10s and t=20s.